UNIVERSITY OF
DENVER

Natural Sciences, Mathematics
and Engineering
Office of the Dean
Boettcher Center West, Room 128
2050 E. Iliff Ave.
Denver, CO 80208
303.871.2693
Fax 303.871.3223

June 26, 2000

Dr. Michael R. Berman
Program Director, Molecular Dynamics
AFOSR/NL
801 North Randolph Street
Room 732
Arlington, VA 22203-1977

Re: F49620-97-0036, "Physical Chemistry of Energetic Nitrogen Compounds"

Dear Dr. Berman:

I have enclosed copies of the Final Report for our program "Physical Chemistry of Energetic Nitrogen Compounds", for which the technical effort was completed on 29 February 2000. I am very grateful to AFOSR for its support of this program, as are the students and faculty colleagues who participated in the work. A number of significant discoveries were made that we hope will benefit both the Air Force and the molecular dynamics research community.

Please contact me if you should have any questions concerning the results described in this report.

Sincerely,

Robert D. Coombe
Professor

REPORT DOCUMENTATION PAGE

AFRL-SR-BL-TR-00-

0300

1. REPORT DATE (DD-MM-YYYY)	2. REPORT TYPE	3. DATES COVERED (From - To)
26-06-2000	Final Report	01-Dec-96 to 02-29-2000

4. TITLE AND SUBTITLE

Physical Chemistry of Energetic Nitrogen Compounds

5a. CONTRACT NUMBER

5b. GRANT NUMBER
F49620-97-0036

5c. PROGRAM ELEMENT NUMBER

5d. PROJECT NUMBER

5e. TASK NUMBER

5f. WORK UNIT NUMBER

6. AUTHOR(S)

Robert D. Coombe

7. PERFORMING ORGANIZATION NAME(S) AND ADDRESS(ES)

Department of Chemistry and
Biochemistry

University of Denver

8. PERFORMING ORGANIZATION REPORT NUMBER

9. SPONSORING / MONITORING AGENCY NAME(S) AND ADDRESS(ES)

Air Force Office of Scientific Research
Chemistry and Life Sciences
801 North Randolph St., Room 732
Arlington, VA 22203-1977

10. SPONSOR/MONITOR'S ACRONYM(S)
AFOSR/NL

11. SPONSOR/MONITOR'S REPORT NUMBER(S)

12. DISTRIBUTION / AVAILABILITY STATEMENT

APPROVED FOR PUBLIC RELEASE: DISTRIBUTION UNLIMITED

13. SUPPLEMENTARY NOTES

14. ABSTRACT

This report describes progress made during a 39-month research program that investigated the NCl/I laser system, the deposition of nitride films from group III azides, and the dynamics of near-resonant laser sputtering. Significant results included the evaluation of excited NF as an energy carrier for atomic iodine lasers, measurement of the rate of energy transfer between vibrationally excited nitrogen and chlorine azide and development of a model for the chain decomposition of chlorine azide, the deposition of boron nitride and gallium nitride thin films from boron and gallium azide precursors, the identification of NNBN as the product of boron triazide decomposition and a likely building block for BN films, and the observation of thermal energy charge transfer in the near-resonant laser sputtering of zinc atoms.

15. SUBJECT TERMS

Azides, Nitride, Boron and Gallium

16. SECURITY CLASSIFICATION OF:			17. LIMITATION OF ABSTRACT	18. NUMBER OF PAGES	19a. NAME OF RESPONSIBLE PERSON
a. REPORT	b. ABSTRACT	c. THIS PAGE			Robert D. Coombe
unclassified	unclassified	unclassified		24	19b. TELEPHONE NUMBER (Include area code) 303-871-2693

INTRODUCTION

This report describes the results of research performed during the period 1 December, 1996 through 29 February, 2000 under the auspices of AFOSR grant number F49620-97-1-0036. The research program, "Physical Chemistry of Energetic Nitrogen Compounds, has been in operation for a number of years and has as its global objectives the development of a better understanding of the mechanisms of energy storage in highly energetic, metastable molecules and the dynamics of processes that occur when such molecules are stimulated by photolysis, reaction, or collisional energy transfer. Much of the research that has been performed under the aegis of this grant has involved the study of energetic nitrogen-containing molecules like azides, isocyanates, amines, and related nitrene, aminyl, and azido radicals.

During the past three years (the period of the grant noted above), the research was focused on two major areas which were investigation of chemical systems relevant to the AGILE laser system (the all gas phase iodine laser) and the deposition of thin films of group III nitrides from the dissociation of energetic group III azides. Both of these areas are related to applications of considerable interest to the U.S. Air Force. A smaller effort was directed toward a third research area that involved study of the mechanism of near-resonant laser sputtering.

The current form of the AGILE laser is based on energy transfer from electronically excited $NCl(a^1\Delta)$ to iodine atoms. In an AGILE device recently demonstrated[1] at the Air Force Research Laboratory at Kirtland AFB, the excited NCl is obtained from the reaction of Cl atoms with N_3 radicals. This reaction was studied in our laboratory some years ago in experiments which led to the first experimental observation of the $NCl(a^1\Delta)$ state[2]. Alternative methods for the generation of excited NCl include[3,4] the dissociation of ClN_3 and the reaction of H atoms with NCl_3. The dissociation of ClN_3 was used in our laboratory for the demonstration[5] of a pulsed AGILE laser in 1995. In this system, mixtures of ClN_3, CH_2I_2, and diluent were irradiated with the output of a pulsed ArF laser at 193 nm to produce both $NCl(a^1\Delta)$ and iodine atoms. Pulsed lasing on the $I\ 5^2P_{1/2} \rightarrow 5^2P_{3/2}$ transition at 1.315 μm was observed, delayed from the photolysis pulsed by several hundred μs. The results were interpreted as indicating the removal of ClN_3 (an efficient I* quencher) from the system by a chain process. The data were analyzed by constructing a kinetic model for the chain that involved propagation by chain carriers $NCl(a^1\Delta)$ and $N_2(v)$. Rate constants for a number of the key processes in the chain were unknown. Measurement of these rate constants and the assembly of a better model for the chain has been one of the major projects of the current research program, with the objective of evaluating the potential the ClN_3 system may have to drive a larger scale device.

Our work on group III nitride films began several years ago when we found a simple gas phase synthesis[6] for the energetic molecule boron triazide that involves the reaction of BCl_3 with HN_3. $B(N_3)_3$ can be dissociated thermally or photolytically and our initial experiments indicated that it has great potential as a "single source" precursor for BN films. In the current program, our efforts were focused on evaluating different means for dissociation of the molecule and developing optimum techniques for film deposition. Considerable progress has been made toward this end. In addition, we completed a first exploration of an analogous chemical system that produces thin films of GaN. This

material has generated great interest since the demonstration in 1996 of a GaN diode laser device operating in the blue-green region[7].

Near-resonant laser sputtering is a process discovered in our laboratory some years ago[8] under the auspices of a previous AFOSR grant[9]. As in conventional laser sputtering, photons from a pulsed laser sputter metal from a target into a reactive gas over the target surface. The uniqueness of our method is that the wavelength of the sputtering laser is nearly resonant with transitions in the metal atoms, such that the atoms are excited to metastable electronic states that react much more rapidly with the reagent gas. The method was originally applied to the preparation of films of ZnO, and resulted in deposition rates nearly an order of magnitude greater than for sputtering with non-resonant photons. The project performed in the current program sought to explore the mechanism of this process.

A number of individual projects were performed within each of these research areas. Much of the work has been published or is in press at the present time, and so we present below only a brief description of each project, the results, and their significance.

Part I. The $NCl(a^1\Delta)/I^*$ Laser System

1. Excitation of I^* by $NCl(a^1\Delta)$ and $NF(a^1\Delta)$

In 1995, shortly after the demonstration of the $NCl(a^1\Delta)/I^*$ laser device in our laboratory[5], a project was undertaken to ascertain whether $NF(a^1\Delta)$ would excite I^* as does $NCl(a^1\Delta)$. Measurements were made with a discharge flow reactor in which F atoms were produced by a microwave discharge through F_2, and Cl atoms were produced in a known proportion by admitting DCl to the flow. Admission of HN_3 produced a mixture of NCl(a) and NF(a) characteristic of the competition between the F and Cl atoms present for the available N_3. Iodine atoms were generated by admitting a very dilute flow of I_2, and the enhancement of the I^* emission intensity upon increasing the NCl(a)/NF(a) ratio was observed. These data were discussed in the final report for a previous AFOSR grant[10]. Interpretation of the data requires the use of an extensive kinetic model for the system. Over the course of roughly 18 months after acquisition of the data, this model was assembled, extended and refined a number of times. Much of this was done by electronic communication with Dr. Amy Hunter, who left our lab (graduating with a Ph.D.) shortly after acquiring the data. The sensitivity of the outcomes of the model (obtained from numerical integration of the coupled differential rate equations with the ACCUCHEM code) to the presence of different rates was determined. The final model included the 48 elementary reactions shown in Table I.

Table I. Kinetic Model for the Excitation of Iodine Atoms by $NF(a^1\Delta)$ and $NCl(a^1\Delta)$

No.	Reaction	Rate Constant (cm^3s^{-1})
1	$F + I_2 \rightarrow IF + F$	4.3×10^{-10}
2	$Cl + I_2 \rightarrow I + ICl$	5×10^{-10}

3	$F + DCl \rightarrow DF + Cl$	1.6×10^{-11}
4	$F + Cl_2 \rightarrow ClF + Cl$	1.6×10^{-10}
5	$F + ICl \rightarrow IF + Cl$	3.8×10^{-10}
6	$F + ICl \rightarrow ClF + I$	1.2×10^{-11}
7	$F + HN_3 \rightarrow HF(v) + N_3$	1.2×10^{-10}
8	$F + N_3 \rightarrow NF(a) + N_2$	5.2×10^{-11}
9	$F + N_3 \rightarrow NF(b) + N_2$	5.8×10^{-12}
10	$Cl + N_3 \rightarrow NCl(a) + N_2$	2.5×10^{-10}
11	$Cl + N_3 \rightarrow NCl(b) + N_2$	2.8×10^{-11}
12	$Cl + HN_3 \rightarrow HCl + N_3$	9.8×10^{-13}
13	$NF(a) + I \rightarrow NF(X) + I$	fit
14	$NF(a) + I \rightarrow NF(X) + I^*$	fit
15	$NCl(a) + I \rightarrow NCl(X) + I^*$	1.8×10^{-11}
16	$NF(a) + CO_2 \rightarrow NF(X) + CO_2$	6×10^{-17}
17	$NF(a) + ClF \rightarrow NF(X) + ClF$	7.6×10^{-12}
18	$NF(a) + I^* \rightarrow NF(b) + I$	5×10^{-11}
19	$2NF(a) \rightarrow N_2 + 2F$	5×10^{-12}
20	$NF(a) + IF \rightarrow NF(X) + IF$	1×10^{-10}
21	$NF(a) + ICl \rightarrow NF(X) + ICl$	5×10^{-11}
22	$NF(a) + I_2 \rightarrow NF(X) + I_2$	1×10^{-10}
23	$NF(a) + HF(v) \rightarrow NF(b) + HF$	1×10^{12}
24	$NCl(a) + CO_2 \rightarrow NCl(X) + CO_2$	4×10^{-13}
25	$NCl(a) + HF \rightarrow NCl(X) + HF$	8.2×10^{-13}
26	$NCl(a) + Cl_2 \rightarrow NCl(X) + Cl_2$	2×10^{-11}
27	$NCl(a) + ClF \rightarrow NCl(X) + ClF$	1×10^{-13}
28	$2NCl(a) \rightarrow N_2 + 2Cl$	4×10^{-12}

29	$NCl(a) + IF \rightarrow NCl(X) + IF$	1×10^{-10}
30	$NCl(a) + I_2 \rightarrow NCl(X) + I_2$	1×10^{-10}
31	$NCl(a) + HCl \rightarrow NCl(X) + HCl$	4.9×10^{-12}
32	$NCl(a) + DCl \rightarrow NCl(X) + DCl$	4.9×10^{-12}
33	$NCl(a) + ICl \rightarrow NCl(X) + ICl$	1×10^{-10}
34	$I^* + CO_2 \rightarrow I + CO_2$	5×10^{-16}
35	$I^* + HF \rightarrow I + HF$	2.7×10^{-12}
36	$I^* + DF \rightarrow I + DF$	1×10^{-14}
37	$I^* + DCl \rightarrow I + DCl$	4.3×10^{-15}
38	$I^* + IF \rightarrow I + IF$	3×10^{-11}
39	$I^* + I_2 \rightarrow I + I_2$	3.6×10^{-11}
40	$I^* + ClF \rightarrow I + ClF$	1.3×10^{-13}
41	$I^* + ICl \rightarrow I + ICl$	1.5×10^{-11}
42	$I^* + Cl_2 \rightarrow I + Cl_2$	1.7×10^{-14}
43	$HF(v) + CO_2 \rightarrow HF + CO_2$	1×10^{-11}
44	$NCl(b) + CO_2 \rightarrow NCl(a) + CO_2$	5.3×10^{-13}
45	$NCl(b) + HF \rightarrow NCl(a) + HF$	1.8×10^{-12}
46	$NCl(b) + ClF \rightarrow NCl(a) + ClF$	1×10^{-12}
47	$NF(b) + I \rightarrow NF(a) + I^*$	3.2×10^{-11}
48	$NF(b) + IF \rightarrow NF(a) + IF$	1.4×10^{-12}

In general, the results showed very clearly that excitation of I* by NF(a) is very inefficient indeed. Setser[11] has reported that the quenching of NF(a) by iodine atoms occurs with a rate constant (at room temperature) of 1×10^{-11} cm^3/s. Our data show that the branching fraction to I* in this process is surely less than 5% (from the accumulated uncertainties of the data), and probably less than 1%. Hence, it is apparent that NF(a) cannot be used to pump an I* laser. Further, the data offer insight into the relative efficiencies with which the $F + N_3$ and $Cl + N_3$ reactions produce excited NF(a) and NCl(a), respectively. In the model, the branching fractions to excited $a^1\Delta$ products were set at 0.9 for both reactions. While the branching fraction for the $F + N_3$ reaction is known[12] to be near this value, that for $Cl + N_3$ was thought to be high but had not been

explicitly measured at the time of this work. From the model and a calibration of the relative sensitivity of the detection system to emissions from NF(a) and NCl(a), we were able to determine a value of 0.53 s^{-1} for the radiative rate of the NCl $a^1\Delta \rightarrow X^3\Sigma^-$ transition, very near the theoretical value[13]. This result suggests that the branching fraction in Cl + N_3 is indeed very high, and in fact recent experiments[14] have placed its value near 0.7. These data also were relevant to a controversy surrounding the Cl + N_3 rate constant, which Setser and co-workers[15] reported to be near that for F + N_3, in contrast to a previous measurement from our laboratory[16] which indicated that k (Cl + N_3) = 5.6 k (F + N_3). The model in Table I includes the factor of 5.6, and the reasonable results obtained lent support to the greater value for k (Cl + N_3) obtained in our earlier work.

Shortly after we had assembled the model shown in Table I and applied it to the data obtained earlier, considerable discussion arose concerning the values of some of the rate constants for quenching processes. Apart from the issue of the Cl + N_3 rate constant noted above, Setser and co-workers reported much smaller rate constants for NCl($^1\Delta$) quenching by a host of species based on data obtained from discharge-flow experiments[17]. Larger values for these rate constants had been obtained in our lab from pulsed experiments in which the excited NCl(a) was produced from ClN_3 photolysis. These photolysis results (i.e., the larger rate constants) had been reproduced by Henshaw and co-workers[18] at the AFRL. To explore this issue, we continued to model the F/Cl/HN_3/I system using both sets of rate constants, and the results are shown in Figure 1.

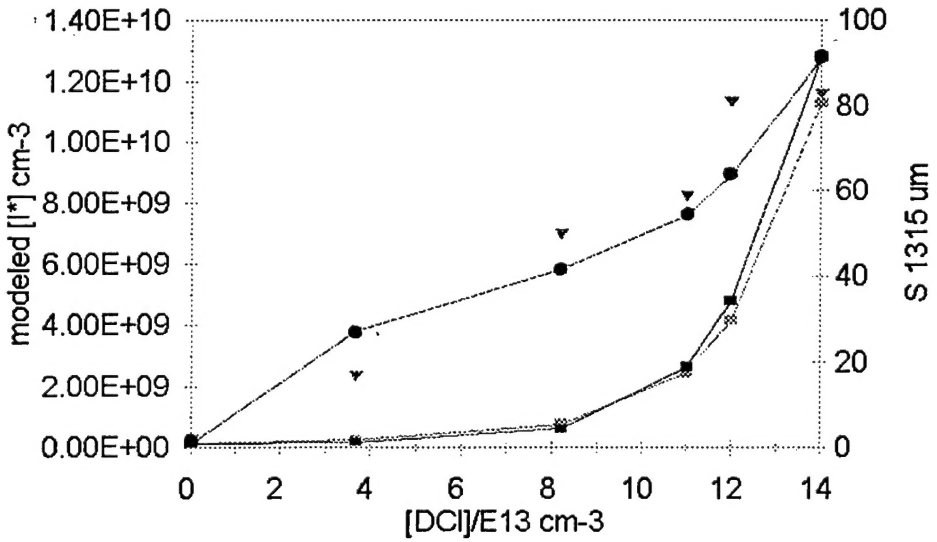

Figure 1. Experimental I* signal and modeled densities of I* vs. the density of DCl added to the flow. Triangles are experimental data; dark circles are from the model with the larger Cl + N_3 rate constant and larger quenching rate constants, the dark squares are from the model with the smaller Cl + N_3 rate constant and the smaller quenching rate constants: the light squares are from the model with the larger Cl + N_3 rate constant and the smaller quenching rate constants.

The figure shows a plot of the enhancement in the I* signal as DCl is added to the flow to create Cl atoms. The data were modeled with rate packages which used the larger Cl + N_3 rate constant and the larger quenching rate constant, the smaller Cl + N_3 rate constant and the smaller quenching rate constants, and combinations of the larger/smaller Cl + N_3 rate constant and the smaller/larger quenching rate constants. In general the best results were obtained with the larger Cl + N_3 rate constant and the larger quenching rates (see

Figure 1), but the smaller Cl + N_3 rate constant and smaller quenching rates also gave reasonable agreement for higher Cl atom densities. Hence, these data are insufficient to resolve the controversy over these rates. What is certain, though, is the effieciency of I* production from $NF(a^1\Delta)$ + I collisions. The I* branching fraction for this process was still found to be less than 5%, for either the larger or smaller rate constants.

2. Energy Transfer from $N_2(v)$ to ClN_3 and the Chain Decomposition of Chlorine Azide

A number of authors[19] have speculated that the chain dissociation of azides is carried by vibrationally excited N_2. This assertion is based on near-resonance between the N_2 vibrational frequency, 2331 cm^{-1}, and the frequency of the most intense feature in the IR spectra of azides, the N_3 "asymmetric stretching " frequency near 2100 cm^{-1}. For higher vibrational levels in N_2, which might well be produced by decomposition of the azides, the energy defect can be near zero. Such a possibility was invoked in our original model for the chain decomposition of ClN_3 in the pulsed $NCl(a^1\Delta)/I^*$ laser demonstration[5], which was based on the production of excited NCl by the chain. In the course of the this AFOSR program, a number of experiments were performed in an effort to test this hypothesis and further evaluate the chain decomposition of ClN_3 as a source of $NCl(a^1\Delta)$.

The first of these was directed toward measurement of the rate constant for vibrational energy transfer between $N_2(v)$ and ClN_3:

$$N_2(v=1) + ClN_3(\nu_2, v=0) \rightarrow N_2(v=0) + ClN_3(\nu_2, v=1) + 281\ cm^{-1} \qquad (1)$$

An apparatus was assembled in which a standard flow reactor was fitted with a high energy dc discharge. The discharge was operated on mixtures of He and N_2, at currents near 300 mA. Gases flowing out of the discharge were passed through a fine Ni mesh to remove N atoms and electronically excited species. The mesh effectively quenched the N_2 first positive emission produced by N atom recombination. The $N_2(v)$ produced in the discharge passed downstream through the mesh and was observed by addition of trace quantities of CO_2 to the flow, such that near-resonant energy transfer between these species[20] produced readily observable emission from vibrationally excited $CO_2(\nu_3)$ near 4.3 μm. This emission was chopped prior to passing through a narrow bandpass filter en route to a cooled InSb detector. The response of the detector was recorded with a lock-in amplifier. For very small densities of CO_2 relative to $N_2(v)$, the time profile of the intensity of the CO_2 emission tracks the time profile of the $N_2(v)$ density in the system. Hence, the rates of $N_2(v)$ quenching by various added species can be determined by monitoring the time decay of the emission from the CO_2 tracer. Figure 2 shows a plot of the natural log of the intensity of the CO_2 emission vs. the density of added ClN_3, recorded at a fixed position 18 ms downstream of the ClN_3 injector. These data indicate that the rate constant for energy transfer from $N_2(v=1)$ to ClN_3 (reaction 1 above) is k_1 = $(2\pm1) \times 10^{-13}$ cm^3s^{-1} at 300K.

This value for k_1 is entirely consistent with the predictions of the Sharma-Brau theory for vibrational energy transfer[21], which suggests that the value of the rate constant should vary as an exponential in the energy defect/kT for $\Delta\varepsilon > 20$ cm^{-1}. The rate constant for energy transfer[21] from $N_2(v=1)$ to CO_2 (which has an energy defect of +18 cm^{-1}) is 5.8 x

10^{-13} cm^3s^{-1}. Using this value as a benchmark, the rate constant for reaction (1) above (with an energy defect of 281 cm^{-1}) is predicted to be 1.5 x 10^{-13} cm^3s^{-1}, clearly within the uncertainty limits of the experimental measurement.

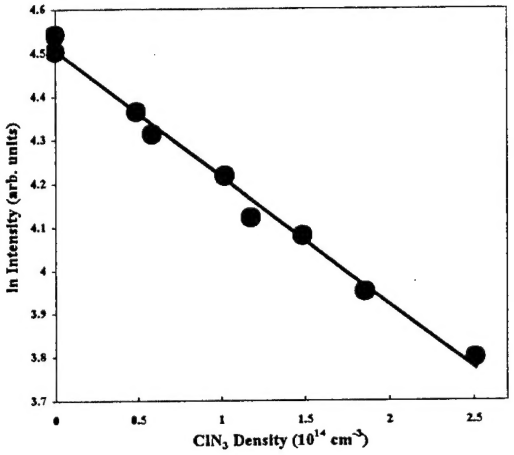

Figure 2. Natural log of the intensity of emission from CO_2 vs. the density of ClN_3.

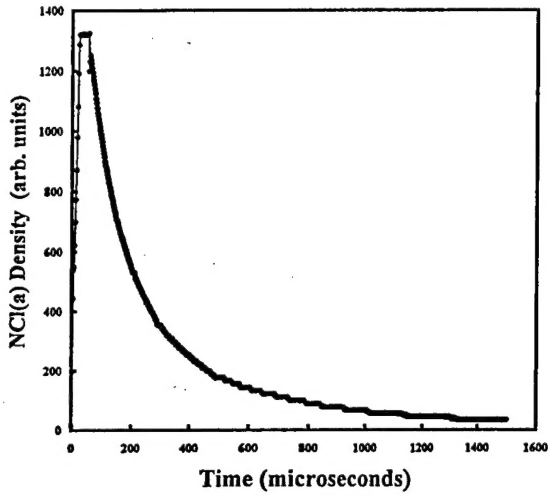

Figure 3. Time profile of the emission from NCl(a), for an initial ClN_3 density of 6.44 x 10^{15} cm^{-3}.

The operation of the ClN_3 chain was investigated in a series of pulsed experiments in which samples of ClN_3 diluted in He were photolyzed at 249 nm with a pulsed KrF laser. The laser fluence in these experiments was kept low such that the maximum dissociation of ClN_3 by the laser pulse was 2.7% of samples that ranged in density from 3 x 10^{15} to 1.6 x 10^{16} cm^{-3} in ClN_3. Emission at 1.077 μm from NCl($a^1\Delta$) was observed subsequent to the laser pulse, and Figure 3 shows a typical NCl($a^1\Delta$) time profile. The profile indicates a fast decay over roughly 200 μs followed by a much slower decay over more than 2 ms. A new feature of these experiments was that the loss of ClN_3 from the system was also observed, via the infrared absorbance of this species at 2050 cm^{-1}. These measurements were made using a broadband IR source to irradiate the sample with detection using a narrow bandpass interference filter and cooled InSb detector. Absorbance values were carefully (and repeatedly) calibrated against absolute ClN_3 densities measured by UV absorbance[22]. Reductions in the IR absorbance of the ClN_3 samples subsequent to the 249 nm laser pulses could then be related to transient reductions in the ClN_3 densities. A typical series of data for different initial ClN_3 densities is shown in Figure 5. It is evident from these data that the removal of the azide from the system continues for several hundred μs after the photolysis pulse, indicating a reaction mechanism. Further, the initial rapid reduction in the ClN_3 density tracks the time decay of the NCl($a^1\Delta$) emission, suggesting a link between these two processes.

Evidence of the nature of this link is shown in Figure 5, a typical time profile of infrared emission observed from vibrationally excited ClN_3 (ν_2). This emission was observed by blocking the broadband IR source and recording the transient emission at 2050 cm^{-1} using the filter and InSb detector noted above. The rise of the emission tracks the initial loss of ClN_3 ($\nu_2 = 0$) from the system (Figure 4) and initial fast component of the time decay of the NCl($a^1\Delta$) emission (Figure 3). All of these data are consistent with

rapid energy exchange between the NCl($a^1\Delta$) photoproduct and the residual parent ClN_3 in the system.

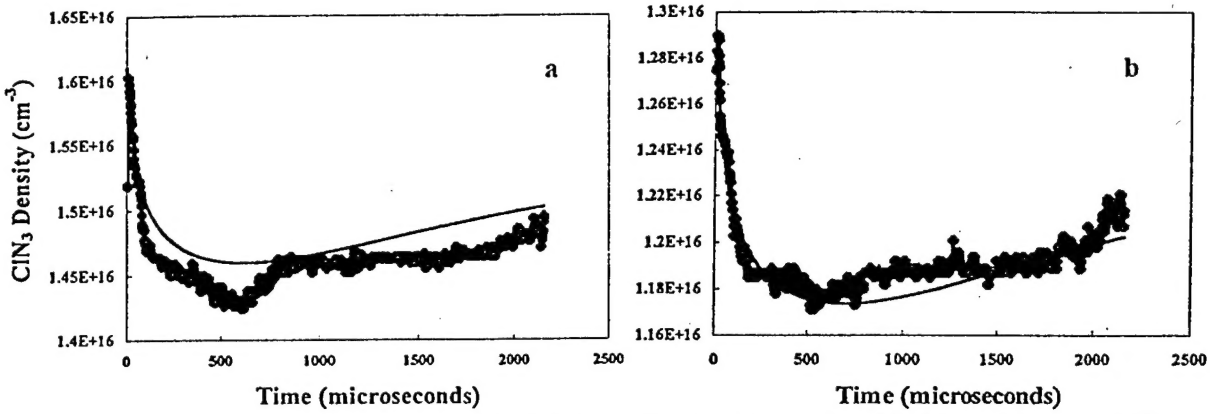

Figure 4. Time profiles of the density of ClN_3(v=0) for photolysis at 249 nm. (a), $[ClN_3]_0 = 1.61 \times 10^{16} cm^{-3}$. (b), $[ClN_3]_0 = 1.29 \times 10^{16}$ cm^{-3}. Solid lines show the results of integration of the kinetic model summarized in Table II.

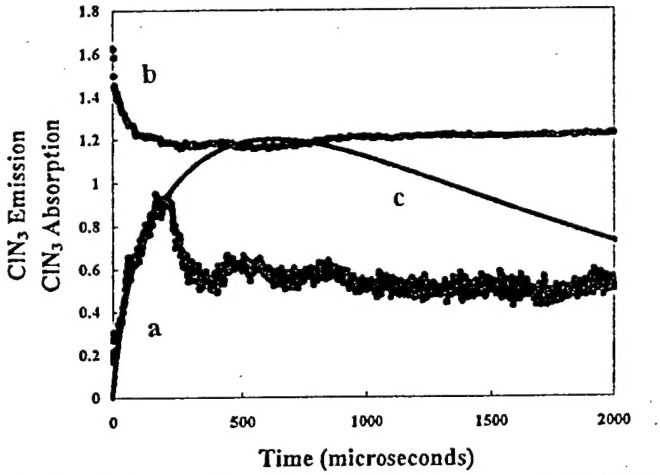

Figure 5. (a) Time profile of IR emission from vibrationally excited ClN_3 for 249 nm photolysis of a sample $[ClN_3]_0 = 1.61 \times 10^{16}$ cm^{-3}. (b) The corresponding time profile of ClN_3(v=0) from IR absorbance. (c) Time profile of ClN_3(v=1) computed from the kinetic model.

The data obtained from the rate constant measurement and from the pulsed experiments were used to assemble a simple kinetic model for the ClN_3 chain decomposition. This model is presented in Table II below. It is assumed that the chain begins with the production of the intermediates NCl($a^1\Delta$) and N_2(v) by the initial photolysis. The chain can be propagated by NCl($a^1\Delta$) as in reactions (2) and (3). Reaction (3) is the electronic-to-vibrational energy exchange noted above, and its rate constant is determined from measurement of the fast initial component of the NCl($a^1\Delta$) for various different ClN_3 densities. This rate constant was in fact found to be dependent on the fluence of the photolysis laser, becoming *slower* at higher fluences. This is surely indicative of the action of processes which regenerate NCl($a^1\Delta$) at higher fluences, and the rate constants obtained for the highest fluences (as small as 6×10^{-13} cm^3s^{-1}) agree with previously published values[18]. Process (2) regenerates NCl($a^1\Delta$) and hence makes no contribution to its observed decay. It does contribute to the removal of ClN_3, though, and its rate constant was obtained from examination of the loss of ClN_3 from the system as observed in data such as that in Figure 4.

Table II. Kinetic Model for the ClN_3 Chain

Initiation

$ClN_3 + h\nu \rightarrow NCl(a^1\Delta) + N_2(v)$	

Propagation

$NCl(a^1\Delta) + ClN_3 \rightarrow NCl(X^3\Sigma^-) + NCl(a^1\Delta) + N_2(v)$	$k_2 = 2.0 \times 10^{-12}$ cm^3s^{-1}
$\rightarrow NCl(X^3\Sigma^-) + ClN_3(v=1)$	$k_3 = 1.5 \times 10^{-12}$ cm^3s^{-1}
$N_2(v) + ClN_3 \rightarrow ClN_3(v=1) + N_2$	$k_1 = 2.0 \times 10^{-13}$ cm^3s^{-1}
$N_2(v) + ClN_3(v=1) \rightarrow ClN_3(v=2) + N_2$	$k_4 = 2.0 \times 10^{-13}$ cm^3s^{-1}
$N_2(v) + ClN_3(v=2) \rightarrow NCl(a^1\Delta) + N_2(v) + N_2$	$k_5 = 2.0 \times 10^{-13}$ cm^3s^{-1}

Termination

$NCl(a^1\Delta) + NCl(a^1\Delta) \rightarrow N_2(v) + 2Cl$	$k_6 = 8.0 \times 10^{-12}$ cm^3s^{-1}
$NCl(a^1\Delta) \rightarrow NCl(X^3\Sigma^-)$	$k_7 = 500$ s^{-1}
$ClN_3(v=1) \rightarrow ClN_3(v=0)$	$k_8 = 500s^{-1}$
$ClN_3(v=2) \rightarrow ClN_3(v=1)$	$k_9 = 2000$ s^{-1}

Chain propagation by $N_2(v)$, reactions 1,4,and 5 is simply too slow to have much of an impact at these densities. Here it is assumed that three quanta of excitation in $ClN_3(\nu_2)$ are needed for dissociation, and that sequential excitation occurs with the rate constant measured for energy transfer from $N_2(v=1)$.

Time profiles of the species in the system were calculated by numerical integration of the differential rate equations corresponding to the reactions in the model, using a fourth order Runge-Kutta routine with variable step size. In general, the results of these calculations agree with the data, and are shown as solid lines in Figures 4 and 5. The model clearly agrees well with the rate of initial ClN_3 loss from the system and with the overall magnitude of this loss, and it also agrees with the time profiles of the initial decay of $NCl(a^1\Delta)$ and the initial rise of $ClN_3(v)$. It does not regenerate the low intensity, slowly decaying component of the $NCl(a^1\Delta)$ time profile, though, (Figure 3) suggesting that it underestimates the degree to which the chain operates under these conditions.

Further, the model in Table II does not predict the behavior of the photo-initiated ClN_3 decomposition at higher fluences. For example, Figure 6b shows the time profile[23] of $NCl(a^1\Delta)$ obtained from the 193 nm photolysis of ClN_3 at an initial density of 7.9×10^{15} cm^{-3}, comparable to that used in the present experiments, but with an initial percentage dissociation of 14%. If the photo-products carry a chain then it should be much more evident in this case, and indeed the emission from the excited NCl is observed to rise to a maximum some 400 μs after the laser pulse, followed by a slow decay over several ms. Figure 6a shows the time profile of I* emission at 1.315 μm from photolysis of a mixture of ClN_3 and CH_2I_2 at 193 nm with a similar fluence and ClN_3 density. Clearly, the I* emission tracks the $NCl(a^1\Delta)$ emission, indicating the operation of the energy transfer process. The model in Table II does not predict the behavior shown in Figure 6b, even if the rate constant for energy transfer from $N_2(v)$ is adjusted upward to account for near-

resonance at higher v levels. For such levels the rate constant should approach that for energy exchange between $N_2(v)$ and CO_2, multiplied by the ratio of the vibrational transition moments[24] in ClN_3 and CO_2 (ClN_3:CO_2 = 4.8). This treatment would suggest that the energy transfer rate constant k_1 might be as large as 2.0×10^{-12} cm^3s^{-1} for these levels. Nonetheless, this is insufficient to reproduce the data shown in Figure 6b. Another possibility is that the chain is branched and hence accelerates rapidly at higher densities of carriers. To test this possibility, we included a phenomenological chain branching reaction in the model, as follows:

$$NCl(a^1\Delta) + ClN_3(v=1) \rightarrow 2NCl(a^1\Delta) + N_2(v=1) \qquad k_{10} = 1.0 \times 10^{-11} cm^3s^{-1}$$

While the operation of such a process is difficult to justify physically, it does represent the creation of three chain carriers from two. Inclusion of the process in the model results in the solid line shown in Figure 6, clearly in reasonable agreement with the data. The value of the rate constant for the branching process (k_{10}) shown above was selected to give the best agreement between the data and the model results.

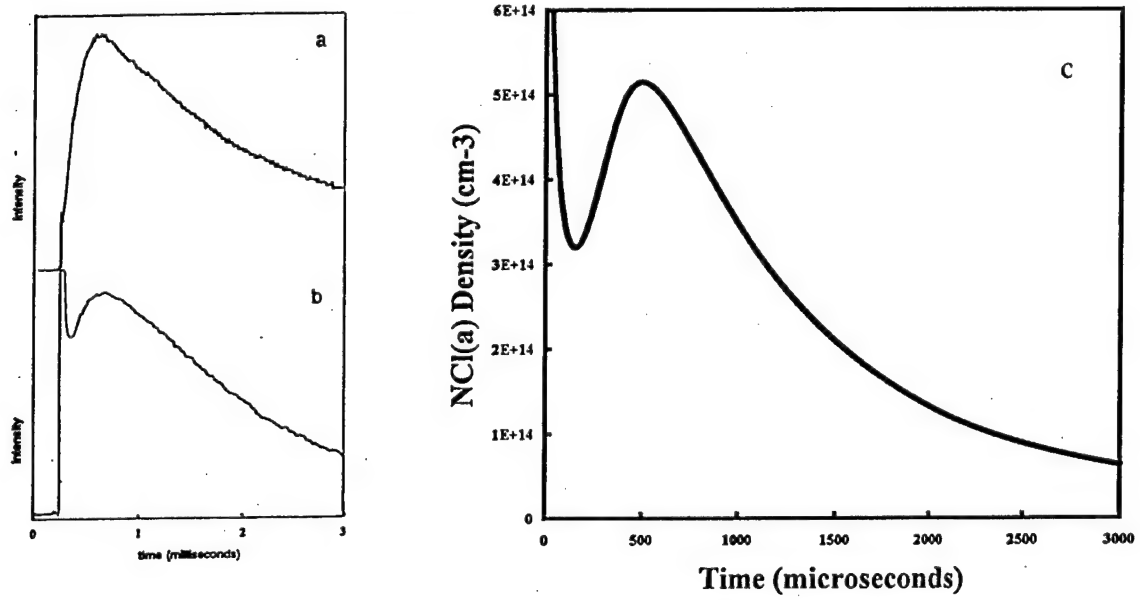

Figure 6. (a) Time profile of I* emission from 193 nm photolysis of a mixture of ClN_3, CH_2I_2, and Ar with 14% initial dissociation of the ClN_3. (b) Time profile of emission from NCl(a) from 193 nm photolysis of a mixture of ClN_3 and Ar, with 14% dissociation of the azide at an initial density of 7.9×10^{15} cm^{-3}. (c) Time profile of NCl(a) emission for conditions as in (b) computed from a kinetic model as shown in Table II, but including the chain branching reaction (10).

In summary, it is clear that the $N_2(v)$ -driven chain decomposition of ClN_3 is far too slow to have an impact at low densities of chain carriers. Our experiments indicate that the chain does operate to a limited extent in this regime, but that it is carried by $NCl(a^1\Delta)$ rather than by $N_2(v)$. $N_2(v)$ may become an important chain carrier at higher densities, but a chain branching reaction (likely one that enhances the generation of $NCl(a^1\Delta)$, as does reaction 10 above) is necessary for this to be the case. Much of this work is described in a manuscript that is to be published in the Journal of Physical Chemistry in July of 2000.

Part II. The Deposition of Group III Nitride Films from Group III Azides

1. Mechanism of the Photochemically Induced Reaction between $Ga(CH_3)_3$ and the Deposition of GaN Thin Films

This project was begun near the end of the previous AFOSR grant[10] and preliminary results were reported in the final report for that grant. A number of additional experiments were performed and the project completed under the present grant. The experiments were begun following our success with analogous reactions of HN_3 with $Al(CH_3)_3$ and BCl_3, which produced azide - substituted Al and B compounds which dissociate upon gentle heating or photolysis to produce AlN and BN films, respectively[6,25]. In the present case, The reaction of HN_3 with $Ga(CH_3)_3$ was found to be very slow, and likely occurs on the vessel walls rather than in the gas phase. This spontaneous room temperature reaction generates CH_4 and azide-substituted Ga compounds, which were observed by their characteristic IR spectra.

Irradiation of the reaction mixture with the 253.7 nm output of a low pressure Hg lamp resulted in a dramatic acceleration of the rate, as shown in Figures 7a and 7b. The reaction produces a film on the cell windows, with an IR spectrum which is shown in Figure 8. The spectrum shows the presence of complexed N_2 (the feature near 2117 cm^{-1}), a feature at 550 cm^{-1} possibly attributable to GaN, and a broad absorption centered near 3300 cm^{-1}. When the film is gently heated (to about 400K), the features at 2117 and 3300 cm^{-1} are lost, and the 550 cm^{-1} feature, now clearly identified as GaN, grows and sharpens.

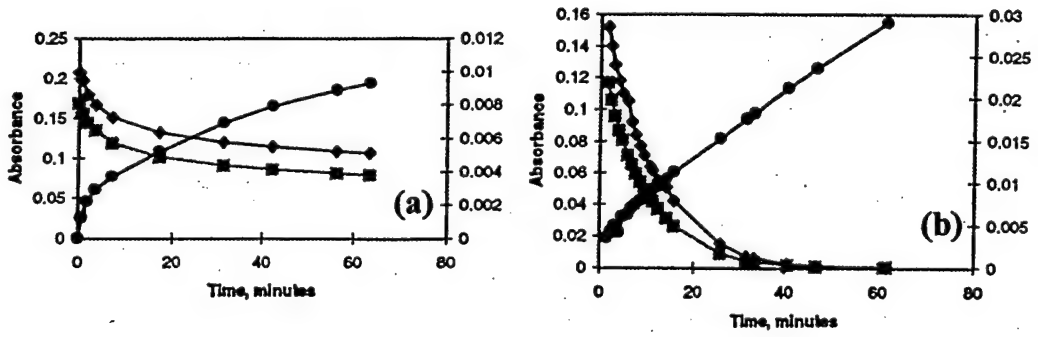

Figure 7. (a) Time evolution of the composition of a gaseous mixture of HN_3, $Ga(CH_3)_3$, and diluent. Squares and diamonds correspond to HN_3 , circles to $Ga(CH_3)_3$. (b) Conditions as in (a) but for a gas mixture irradiated at 243.7 nm.

While $Ga(CH_3)_3$ has a very small absorption at 253.7 nm (and indeed irradiation at this wavelength had no effect on samples of $Ga(CH_3)_3$) alone), it is known that photolysis of HN_3 at wavelengths near 260 nm produces excited $NH(a^1\Delta)$ with a yield near unity[26]. Like its isoelectronic analogues $O(^1D)$ and $CH_2(^1A')$, NH(a) undergoes electrophilic insertion reactions. We believe that the NH(a) produced by the photolysis inserts into the $Ga\text{-}CH_3$ bond of surface-bound $Ga(CH_3)_x$ moieties. The transient $Ga\text{-}NH\text{-}CH_3$ intermediate thus formed would rapidly eliminate CH_4 to leave surface - bound GaN, as indicated by the IR spectra. The NH(a) can also react rapidly with the parent HN_3 to produce NH_2 and N_2, and the NH_2 can react with HN_3 to generate NH_3. The broad IR

feature centered at 3300 cm^{-1} observed before warming is attributable to incorporation of NH_3 produced in this manner into the film.

The results of this project were published as an article[27] in Applied Physics Letters in 1998.

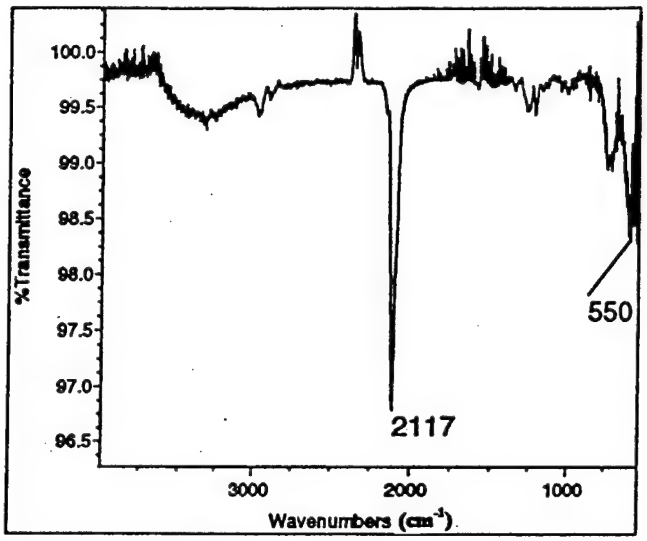

Figure 8. IR spectrum of film produced by the 253.7 nm irradiation of a mixture of HN_3, $Ga(CH_3)_3$, and diluent.

2. Photodissociation of $B(N_3)_3$ in Low Temperature Argon Matrices

As part of the original study of the synthesis and dissociation of $B(N_3)_3$ in our laboratory, the UV/Visible absorption spectrum of this species was measured in the gas phase[6]. The data indicated a very large ($\sigma = 1.3 \times 10^{-17}$ cm^2) absorption near 230 nm. This feature likely corresponds to an $n \rightarrow \pi^*$ transition involving electrons on the azide chains, by analogy with other such compounds, and photolysis should result in rupture of the weak $N\text{-}N_2$ bonds. From the pressure rise observed upon complete photodissociation of known amounts of $B(N_3)_3$, it was concluded that each $B(N_3)_3$ molecule releases three N_2 molecules, suggesting the existence of a BN_3 fragment which might well be the precursor of the BN films observed in our experiments. Subsequently, a number of experiments directed toward isolating and identifying the products of $B(N_3)_3$ photodissociation were performed. This work was done in collaboration with Professor J.V. Gilbert of the Chemistry Department at DU. Professor Gilbert's laboratory has extensive capabilities in the area of low temperature matrix isolation.

The trapping of $B(N_3)_3$ in an Ar matrix near 10K was accomplished at the very end of the previous AFOSR program[10] and this result was described in the final report for that grant. In the present program, trapped $B(N_3)_3$ was successfully photodissociated using a broad -band UV light source (a D_2 lamp). Species trapped in the matrices were identified by FTIR spectroscopy. Upon photolysis, the IR features associated with trapped $B(N_3)_3$ gradually diminished to near zero absorbance. The matrices also contained some unreacted HN_3 and BCl_3, and these were affected very little by the photolysis in keeping with their smaller absorption cross sections in the near UV. Products of the photodissociation of $B(N_3)_3$ were observed to grow into the IR spectra, and were identified by correlating the time dependence of their growth with that of the loss of the parent $B(N_3)_3$. The results of these experiments were very clear. Figure 9

shows IR spectra (sequenced in time) of these products features. The features at 1804, 1861, 1941, and 2101 cm^{-1} clearly grow in with a time dependence that matches that of the loss of the parent azide. Another feature near 2070 cm^{-1} grows in and then diminishes over this same photolysis period.

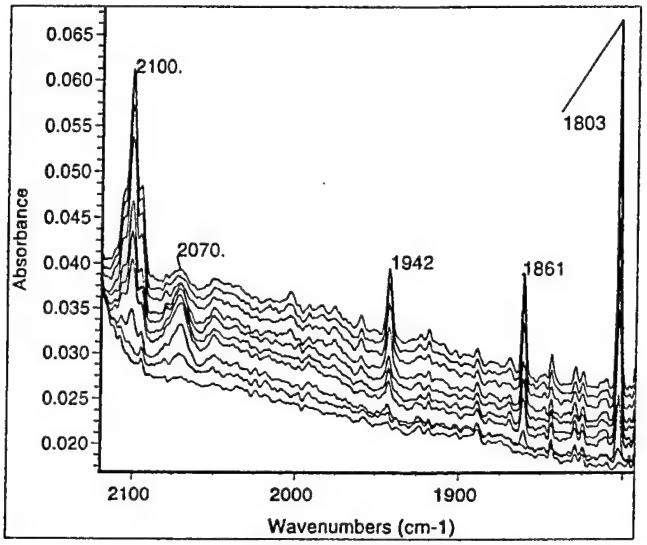

Figure 9. Infrared absorption spectra showing progress of the photodissociation of $B(N_3)_3$ trapped in an Ar matrix near 10 K. Increasing time moves from bottom to top.

If all three N_2 molecules were lost from $B(N_3)_3$ in a concerted manner (a possible, if improbable route), the result would be a trigonal BN_3 fragment. This would likely also be the case if the molecule dissociated by sequential absorption of a number of photons. We performed a number of electronic structure calculations (geometry optimizations with GAUSSIAN 94 [28]) to ascertain the stability of this trigonal BN_3 fragment. As expected it is not stable, and probably rearranges to a boron monoazide molecule (BNNN) or perhaps to NNBN, a species that is isoelectronic to cyanogen (NCCN). The IR spectral data show that the latter is indeed the case. Andrews and co-workers[29] have isolated and identified a number of B_xN_y species produced by laser ablation of boron into gaseous N_2. One of these species is linear NNBN, and its frequencies are reported as 1802.0, 1859.6, and 2091.7 cm^{-1} , clearly matching those in the spectrum shown in Figure 9. The1804 and 1861 cm^{-1} features in our spectrum correspond to the N_2B-N stretching vibration in the molecule with the ^{10}B and ^{11}B isotopes, respectively. These features show the expected frequency splitting and 1:4 intensity relationship characteristic of these isotopes. The 2101 cm^{-1} feature corresponds to the N-NBN stretching vibration in the molecule. The latter is much like the features of complexed N_2 observed in other experiments with Al and Ga compounds[25,27]. The 1941 cm^{-1} feature has not been assigned.

This work on the trapping of $B(N_3)_3$ in a low temperature matrix and the production of NNBN from photolysis was published as an article in the Journal of Physical Chemistry[30].

The identification of the NNBN fragment is a most interesting result for a number of reasons. First, it is very clearly the dominant fragment of the photodissociation, as no other stable product features appear in the IR spectra. If it is indeed like cyanogen, it may have electronic transitions amenable to LIF that might be observed subsequent to photodissociation in the gas phase. If so, we can study the detailed dynamics of the

$B(N_3)_3$ photodissociation process. Second, if it is the dominant (or only) dissociation fragment (apart from N_2), then *it must be the precursor of the BN films that result.* The hexagonal and cubic morphologies of these films should then arise from different modes of self-assembly of the NNBN fragments. For example, one can imagine hexagonal BN arising from assembly of linear NNBN species on a planar surface. To investigate this issue, a number of computations of the energetics of such self-assembly processes were performed using the GAUSSIAN 94 [28]. From the computed charge distribution along the backbone of isolated linear NNBN molecules[30], potential energy curves were calculated for two molecules approaching one another to form a dimer, then for addition of a third molecule to form a trimer, and finally for ring closure to form a borazine ring, the basic unit of hexagonal BN. Figure 10 shows these potential energy curves and the associated structures. It is clear that while all three steps are favored by attractive potentials, the first step (dimer formation) is most difficult (with the hint of a barrier in the entry channel). The subsequent trimer and ring structures are strongly bound. In the curves, the parameter R corresponds the distance along the bond being formed. The calculations were performed at the Hartree-Fock level of theory with a 6-31g(d) basis set. The self-assembly process is based on electron donation from the terminal N atoms into the unoccupied p-type orbitals on the B atoms. The borazole rings characteristic of the hexagonal structure would result from loss of the three N=N moieties. Formation of the cubic (tetragonal) structure would require bending of the linear NNBN molecules, and hence is expected to be a higher energy structure. Still, it might be the case that epitaxial growth of either form from NNBN would require only the appropriate template; for example, cubic BN might be grown if NNBN were deposited (from dissociation of $B(N_3)_3$) over a diamond film. Perhaps some minimal input of energy would be required to sustain the needed surface mobility. These issues were explored in a separate project directed toward BN film deposition, described below.

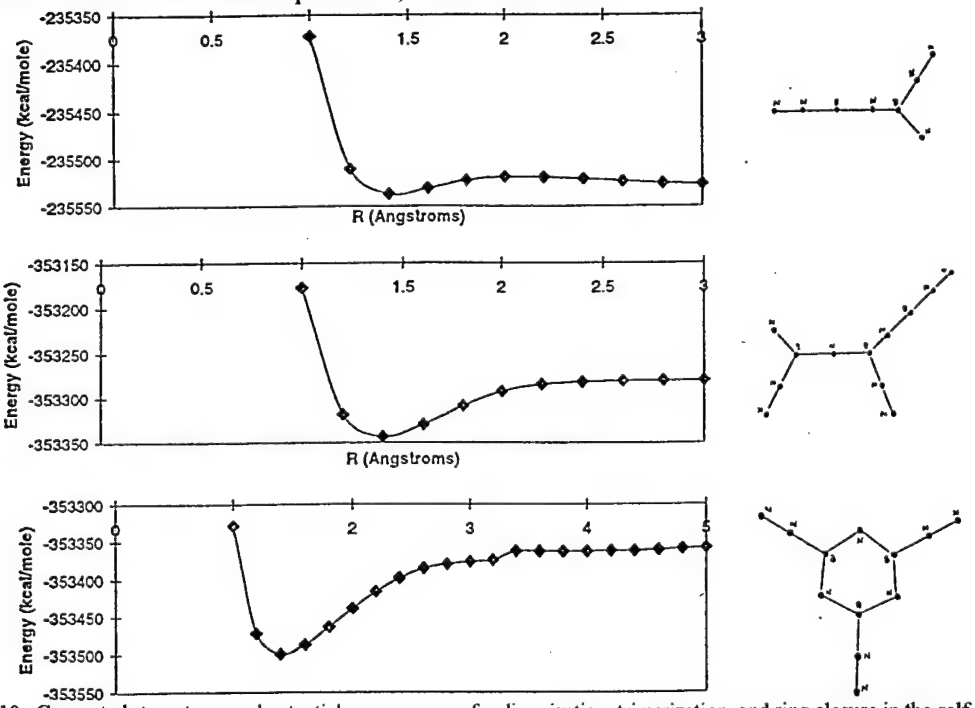

Figure 10. Computed stgructures and potential energy curves for dimerization, trimerization, and ring closure in the self-assembly of NNBN molecules. Structures are shown to the right.

3. Deposition of BN Films from the Dissociation of $B(N_3)_3$

The objective of this project was to explore and develop methods for the deposition of good quality BN films from the dissociation of $B(N_3)_3$, which is believed to proceed to NNBN as above. The basic apparatus used for these experiments went through a number of changes as more information was gathered, and a typical version is shown below in Figure 11. Continuous flows of HN_3 and BCl_3 in the stoichiometric 3:1 ratio are allowed to react in a ballast volume with a retention time adequate for complete reaction. The flowing products of the reaction are analyzed by passage through an FTIR spectrometer. In general, the flowing reaction was quite stable and flows containing no IR active products other than $B(N_3)_3$ were easily obtained. HCl was not observed in the effluent of the reactor, suggesting that it is preferentially removed by the walls of the flow system and ballast volume. Once stable flows of $B(N_3)_3$ were established, they were directed to the deposition chamber via a three-way valve.

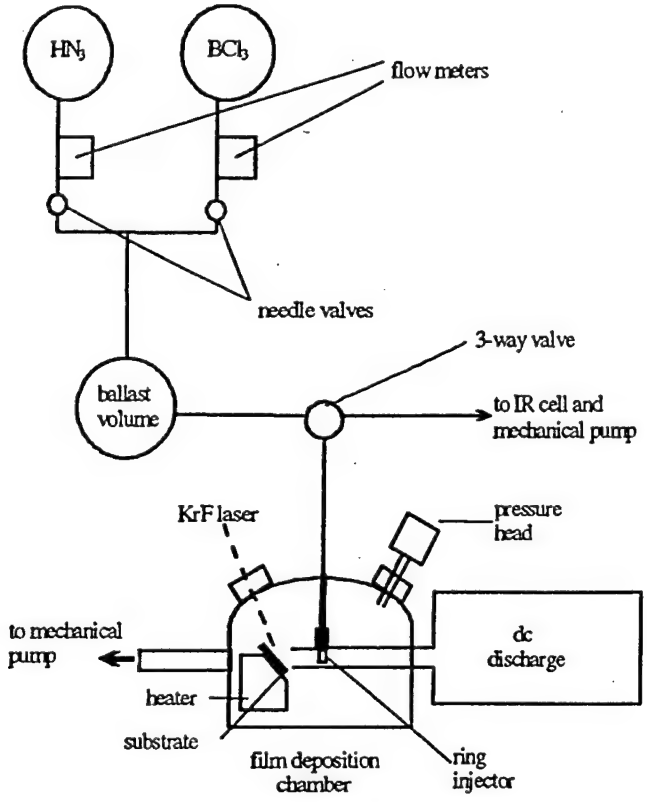

Figure 11. Apparatus used for continuous generation of $B(N_3)_3$ and deposition of BN thin films

In initial experiments, films were deposited by thermal dissociation of the azide parent on KCl, quartz, sapphire, and Ni substrates at temperatures near ambient. Sapphire has a good lattice match with hexagonal BN and the Ni(100) surface is very

well matched[31] to cubic BN. Only very thin films (<100 nm) were deposited in these first experiments. Greater film thickness was achieved by cooling the substrates, but the films had poor chemical quality. The films exhibited the characteristic IR absorption features[32] of hexagonal BN near 1400 and 750 cm^{-1}, but they also showed very large, broad absorptions near 3300 cm^{-1} indicative of hydroxide groups. Indeed, these films were very susceptible to oxidation from tiny air leaks into the system. When the reagent flows were turned off, the films rapidly became chalky white indicative of the oxide. This effect was mitigated somewhat by replacing the reagent streams with a flow of N_2. The oxidized films were soft and had minimal adherence to the substrate surfaces. X-ray analysis indicated the films to be amorphous.

The dc discharge shown in Figure 11 was added to the apparatus based on work reported by Benard and co-workers[33] on the production of C_3N_4 films from the dissociation of NCN_3. These authors reported that cyanogen azide is dissociated by collisions with vibrationally excited $N_2(v)$ produced in a dc discharge, presumably by a sequential excitation mechanism analogous to reactions 1,4, and 5, above. Good quality C_3N_4 films were produced for substrate temperatures above 450 °C. In experiments performed in our laboratory, He and N_2 were passed through a 100 mA dc discharge and the effluent (presumably $N_2(v)$, N atoms, and electronically excited $N_2(A)$ metastables) mixed with $B(N_3)_3$ which entered the flow via a ring injector. This flowing reaction mixture was then directed onto the substrate surface, held at temperatures from ambient (25 °C) to 300 °C. The substrates used in these experiments were sapphire and silicon. The former has a far better lattice match with BN, but the latter allows easy investigation of the chemical composition of films by FTIR transmission spectroscopy. A further improvement that was made allowed for in-situ cleaning of the substrate surface by irradiation with a UV laser. This was done with a pulsed KrF laser (249 nm), with the beam entering the deposition chamber through a fused silica window and irradiating the substrate prior to admission of the $B(N_3)_3$ to the system.

These changes resulted in a much greater deposition rate and much improved film quality. The films produced were purer, with the IR spectra of the films grown on silicon showing no evidence of boron oxides (Figure 12). XPS analyses of BN films grown on both sapphire and silicon (Table III) indicate B:N ratios near 1:1. The XPS spectra also show that carbon and nickel are present in the films as minor impurities, likely from the discharge. Most of these impurities are removed by short sputtering with Ar. Further, the films are more adherent to the substrate surfaces. Analysis of the film morphology by x-ray diffraction was disappointing, though, with all of the data gathered to date indicating that the films grown at low temperatures (room temperature to 200 °C) are amorphous. While this is an expected result for the films grown on silicon, which has a 25% lattice mismatch with BN, we had hoped to see some evidence of polycrystalline structure for the films on sapphire. It seems apparent that while the chemical production of the hexagonal BN moiety can occur at very low temperatures, even at room temperature, energy is still needed to provide the surface mobility necessary for assembly of the reaction intermediates (perhaps NNBN) into polycrystalline structures. Indeed, there may be some threshold surface temperature needed for the onset of longer range order.

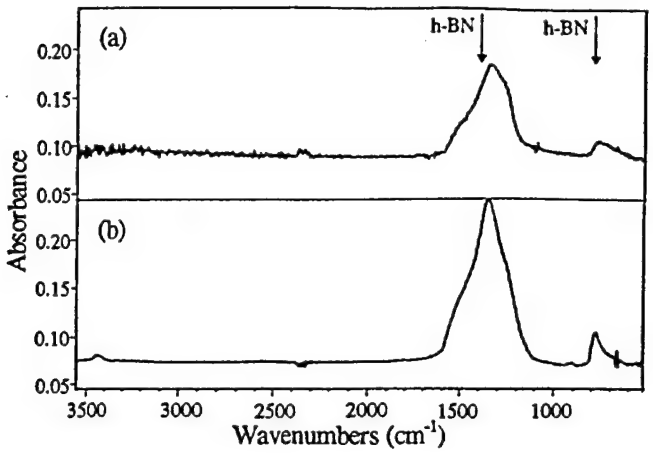

Figure 12. FTIR absorption spectra: (a) film grown on Si at 200° C; (b) film grown on Si at 300° C. Known IR absorption frequencies for hexagonal BN are marked.

Table III. XPS Analysis of Four Different Films

Substrate material	Growth T (°C)	Spectrum area	B 1*s*	Atomic N 1*s*	Concentration (%)[a] O 1*s*	O 1*s*	Cl 2*p*	Ni 2*p*[3]
Silicon	200	Surface	12	11	21	47	4	5
		interior	36	14	44	1	1	3
Silicon	300	Surface	26	24	18	28	3	1
		interior	42	22	29	5	0	1
Sapphire	200	Surface	8	14	20	52	3	3
		interior	22	21	44	10	0	2
Sapphire	300	Surface	20	17	24	32	4	3
		interior	35	21	31	5	3	5

[a]The atomic concentrations are normalized to 100% in each film.

A number of experiments were also performed in an effort to identify the energy carrier in the excited N_2 stream that is responsible for dissociation of the $B(N_3)_3$ in the system. First, the role of vibrationally excited $N_2(v)$, the energy carrier indicated by Benard[33], was tested by inserting a Ni screen into the flow downstream of the discharge. The screen removes N atoms and electronically excited N_2 but not $N_2(v)$. BN films could not be grown with the Ni screen in place, suggesting that $N_2(v)$ is *not* in fact the energy carrier. Next, the possibility that N atoms are the carrier of the reaction was tested by replacing the dc discharge with a 100 W microwave discharge, which is known to make a much greater proportion of atoms (relative to $N_2(v)$) than does the dc discharge. Here too no BN films were generated. Based on these results, it was speculated that the actual energy carrier is metastable $N_2(A^3\Sigma^+_u)$. This is reasonable since these metastables should be present in the dc discharge, and the energy they carry (6.2 eV) is such that excited dissociative states of the azide might be easily accessed by energy transfer. Indeed, $B(N_3)_3$ has a strong optical absorption feature at 230 nm (5.4 eV), and photoexcitation in this band dissociates the molecule, producing NNBN and BN films[6,30]. Further, excitation and dissociation of other azides by $N_2(A)$ metastables is well known[34]. To test this possibility, the apparatus was rearranged such that only Ar passed through the dc

discharge. Either pure N_2 or $B(N_3)_3$ heavily diluted in N_2 was admitted through a ring injector downstream of the discharge, just upstream of the substrate surface. In either case, admission of the N_2 created an easily visible red afterglow, and spectra in the UV and visible regions indicated the first positive and second positive transitions in N_2. These are the emissions expected from interaction with Ar (^3P) metastables[34], and suggest that the dominant excited species in this flow is $N_2(A)$. This configuration (with $B(N_3)_3$ flowing) resulted in the best BN films prepared in our laboratory to date, and hence it is believed that $N_2(A)$ is in fact the agent responsible for dissociation of the azide.

These results and their analysis have been published as an article[35] in the Journal of Applied Physics.

Part III. Dynamics of Near-Resonant Laser Sputtering

The near-resonant laser sputtering effect was first observed in our laboratory under the auspices of a previous AFOSR grant[9]. In those experiments[8], a very significant enhancement in the rate of deposition of ZnO from laser sputtering of Zn into O_2 was observed when a XeCl laser (308 nm) was used instead of a KrF laser (249 nm). This was interpreted as arising from optical pumping of the vapor phase Zn atoms, which have a $4^1S_0 \rightarrow 4^3P_1$ transition at 307.7 nm. Emission from the excited $Zn(^3P_1)$ state was observed in the system, and it was shown that the rate constant for reaction of Zn in this state with O_2 is nearly the gas kinetic value. It was thought that the Zn atoms were able to absorb the non-resonant 308 nm laser radiation because of significant line broadening in the zone near the surface of the Zn target.

This project was directed toward testing this hypothesis. An apparatus was used in which Zn is sputtered from a target either under vacuum or in the presence of added gases. The composition of the sputtered Zn plume is probed by using either emission or LIF methods, and time resolution is obtained by mounting the detection apparatus perpendicular to the direction of travel of the plume. A number of quite interesting results were obtained, some of which suggest that still greater increases in deposition rates might be realized.

The natural radiative lifetime of the $Zn(^3P_1)$ state is 20 μs, and the apparent lifetime of the ^3P level can be extended to 60 μs by equilibration among the $^3P_0$, $^3P_1$, and $^3P_2$ states[36]. Hence it was expected that emission from the $^3P_1$ state would be observed for a maximum of 60 μs after the sputtering laser pulse, and this was indeed the case under vacuum conditions. Further, the density of $^3P_1$ emitters in the plume was several times greater for photolysis at 308 nm vs. 249 nm (for equivalent fluences near 1 J/cm^2), supporting the earlier hypothesis. When small pressures of Ar (20 mTorr and greater) were established in the sputtering chamber, though, much different behavior was observed. Figure 13 shows a time profile of $Zn(^3P_1)$ emission observed for an Ar pressure of 100 mTorr. While the 60 μs peak is still evident, a more intense feature of greater duration is observed after a delay of 500 μs and with a maximum at 700 μs. Since the detector observes the plume in a zone about 3 cm away from the target surface, this feature corresponds to excited Zn atoms moving with considerably less kinetic energy. Further, these atoms must be excited by collisions with an energy carrier that lasts for ms after the

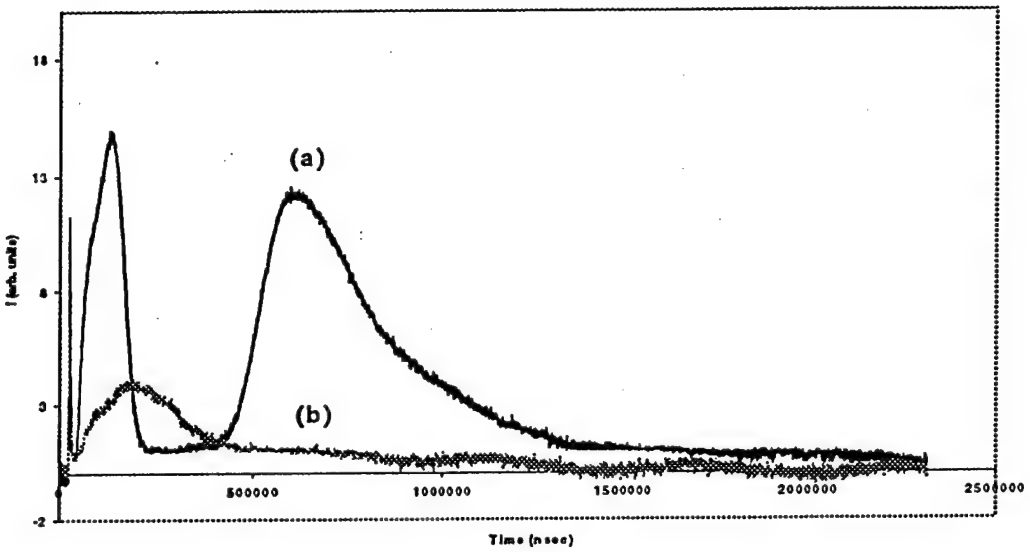

Figure 13. Time profiles of emission from $Zn(^3P_1)$ for sputtering by radiation at (a) 308 nm, (b) 249 nm.

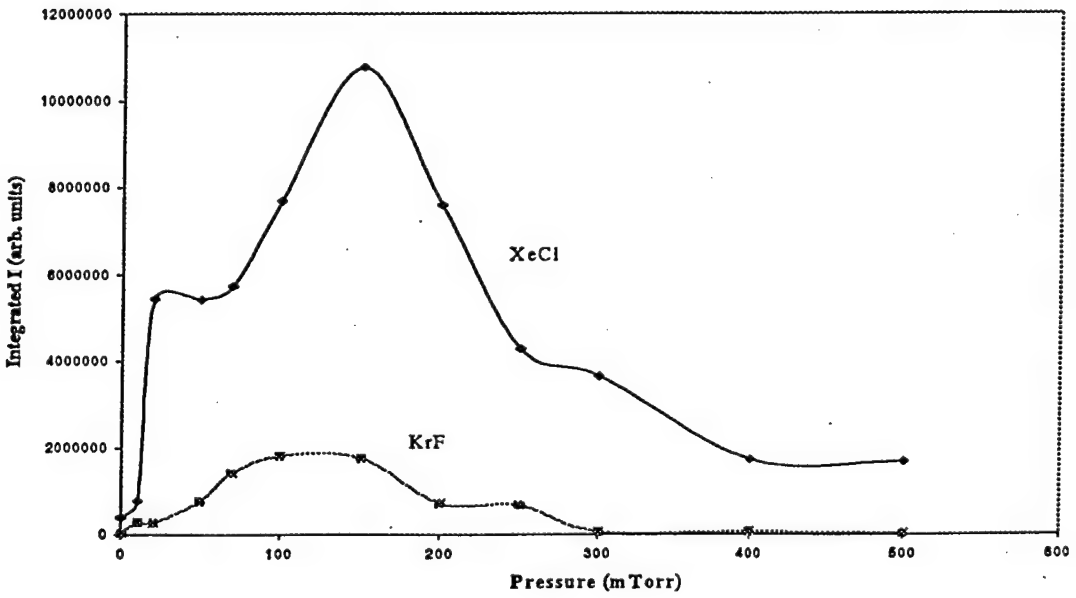

Figure 14. Integrated intensity of $Zn(^3P_1)$ emission from sputtering with XeCl (308 nm) and KrF (249 nm) lasers vs. Ar pressure.

laser pulse. Data such as that shown in Figure 13 were obtained for a wide variety of Ar pressures, laser fluences, and for both 308 nm and 249 nm irradiation of the target. In keeping with the earlier results, the generation of comparable $Zn(^3P_1)$ emission intensity required much greater fluences at 249 nm for all Ar pressures. Figure 14 shows a plot of the emission intensity vs. Ar pressure for both 308 nm and 249 nm sputtering.

An estimate of the density of excited $Zn(^3P)$ atoms in the plume was obtained by recording the spectra of the emission signal. In addition to the $4^3P_1 \rightarrow 4^1S_0$ transition at 307.7 nm, the spectra exhibited the three lines of the $6^3S_1 \rightarrow 4^3P_{0,1,2}$ transition which lie nearby at 301.9, 303.6, and 307.2 nm. The presence of these lines is indicative of the occurrence of a near-resonant energy pooling process as follows:

$$Zn(4^3P_{0,1,2}) + Zn(4^3P_{0,1,2}) \rightarrow Zn(6^3S_0) + Zn(4^1S_0) \qquad (11)$$

From the rate constant for this process, the initial density of $Zn(4^3P_{0,1,2})$ can be calculated from the relative intensities of the atomic lines in the observed spectra. Umemoto and co-workers[37] have reported that the overall rate constant for $Zn(^3P)$ energy pooling is $(7\pm2) \times 10^{-10}$ cm^3s^{-1}, with the formation of excited triplet states favored over formation of excited singlets by a factor of approximately 2. Since energy pooling can also form the $5(^3S_1)$ and $4(^3D_J)$ states, we assume k_{11} has a value near 1.0×10^{-10} cm^3s^{-1}. With this assumption, the density of excited Zn atoms in the plume at a time corresponding to the peak of the second maximum in Figure 13 is inferred to be on the order of 5×10^{13} cm^{-3} for laser fluences on the order of 1 J/cm^2.

Spectra of the plume were also recorded deeper in the UV region and distinct features corresponding to exited Zn^+ ions were observed, as shown in Figure 15. Here again these features (corresponding to the fully allowed $^2P \rightarrow {}^2S$ transition) were observed at times corresponding to the second maximum of the $Zn(4^3P_1)$ emission, several hundred μs after the laser pulse. In fact, the time profile of the Zn^+ emission appeared to correspond to that of the emission from the excited neutral atoms. It is important to note that, like the second maximum in the emission from the neutrals, emissions from the ions were detected only when Ar was present in the system, and not when the system was under vacuum.

We believe that these observations are evidence of the occurrence of a thermal energy charge transfer process ("TECT") between Zn and Ar atoms, as follows:

$$Ar^+(^2P_{1/2,\,3/2}) + Zn(4^1S_0) \rightarrow Ar(^1S_0) + Zn^+(4^2P_{1//2,3/2}) \qquad (12)$$

The occurrence of this process has been suggested by Tamir and Shuker[38] based on observations of emission in Ar/Zn discharges. Process (12) is "near resonant" in the sense that it is exothermic by a few tenths of an eV (the exact energy release is determined by the J levels of the atoms), a small amount relative to the ionization energies of either Zn or Ar. This TECT process may in fact proceed in both directions (i.e., to produce either Zn^+ or Ar^+) if the translational energy of the material ejected into the plume is high. If so, Ar^+ would serve as the long lived energy carrier in the system, with the energy continuously being transferred between Ar^+ and Zn^+. Energy would be lost by radiation from either excited Zn^+ $(^2P_{1/2,3/2})$ or excited $Zn(^3P_1)$. The excited neutrals would be formed by ion-electron recombination, and indeed Tamir and Shuker

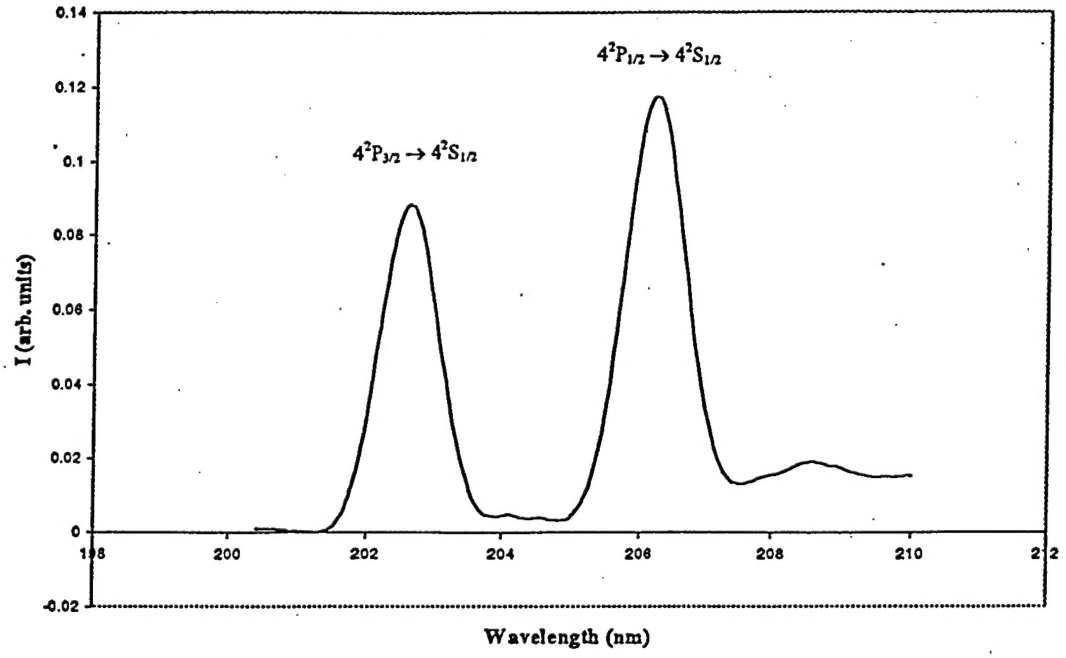

Figure 15. Spectrum of the sputtered plume in the UV region at t = 700 μs, for 308 nm irradiation at 1.5 J/cm^2.

note that the TECT process would result in strong emission from the excited triplet neutrals, as we see in our experiments. This argument is strongly supported by the similar time profiles of the $Zn(^3P_1)$ and $Zn^+(^2P_{1/2,3/2})$ emissions, and by the requirement for the presence of Ar.

The data suggest that the optimum conditions for laser sputtering processes that produce films of Zn, ZnS, and ZnSe would involve the use of 308 nm radiation and the presence of Ar to extend the lifetime of excited species.

CONCLUSIONS AND FUTURE WORK

The principal known means for the generation of excited $NCl(a^1\Delta)$ for pumping NCl/I* lasers are the dissociation of ClN_3, the $Cl + N_3$ reaction, and the reactions of NCl_2 with H or D atoms. This work has investigated the collisional dissociation of ClN_3, and the results indicate that energy transfer from $N_2(v)$ from an external source is likely too slow a process to pump a laser device. Initiation of the chain decomposition of ClN_3 might well produce N_2 in higher vibrational levels for which the energy transfer rate is anticipated to be greater, and may enhance the rates by temperature increases associated with the energy release. Further, chain branching may involve non-linear regeneration of the chain carriers $NCl(a^1\Delta)$ and $N_2(v)$. Our results indicate that such chain branching is likely at higher densities of chain carriers. These reactions are certainly complex and may not be controllable, though. At the present time, the reactions of NCl_2 with H or D atoms appear to offer the best opportunities for improvement over the $Cl + N_3$ system used in the AGILE device currently being studied at AFRL. We have begun a new project directed toward the further evaluation of NCl_2-based $NCl(a^1\Delta)$ generation methods.

Whether driven by photolysis, thermolysis, or collisions it is likely that $B(N_3)_3$ dissociation proceeds through a trigonal BN_3 intermediate that rapidly rearranges to linear NNBN. Our work suggests that BN films produced from $B(N_3)_3$ dissociation are produced by self assembly of these NNBN molecules into the ring structures that characterize hexagonal (sp^2 bonded) BN. Formation of cubic (sp^3-bonded) BN from self assembly of NNBN would require bending of the linear structure of this molecule, and it would be interesting to explore the effect of excitation of this bending mode on the nature of the BN films produced.

The energy stored in $B(N_3)_3$ is such that hexagonal BN films can be deposited by thermolysis at temperatures as low as 300 K. Photolysis and dissociation by collisions with $N_2(A)$ metastables also produce hexagonal films on substrates at temperatures from 300 to 500 K. It is apparent, though, that the energy release in these processes is insufficient to provide the surface mobility needed for the formation of long range order in the films produced. To date only amorphous BN films have been deposited from $B(N_3)_3$, albeit with good chemical quality. It is clear that an additional input of energy at the substrate surface is still needed to generate crystalline or polycrystalline films. We are currently exploring deposition at elevated temperatures and low energy plasma deposition of BN films in an effort to quantify this energy requirement. In light of the data obtained in the present program, it still seems that $B(N_3)_3$ offers a great opportunity for the low energy deposition of BN films with good chemical quality. Relative to other "single precursor" molecules, it is truly unique in that it is comprised of only B and N atoms with a large excess of nitrogen. Further, the notion of "building" BN films from the self assembly of NNBN, and the possibility of controlling this process, is most appealing.

We believe that the thermal energy charge transfer mechanism is the underlying cause of the near-resonant laser sputtering effect observed in our laboratory some years ago. The present results further clarify the optimum conditions for Zn sputtering to include both the use of near-resonant 308 nm laser radiation (from a XeCl laser) and the presence of Ar to effect the TECT process. This method holds the promise of significant improvements over the plasma deposition methods typically used for deposition of ZnO and similar compounds.

PUBLICATIONS ARISING FROM THIS WORK

1. C.J. Linnen and R.D. Coombe, "Mechanism of the Photochemically Induced Reaction Between $Ga(CH_3)_3$ and HN_3 and the Deposition of GaN Thin Films", Appl. Phys. Lett., **72**, 88 (1998).
2. I.A. Al-Jihad, B. Liu, C.J. Linnen, and J.V. Gilbert, "Photodissociation of $B(N_3)_3$ in Low Temperature Ar Matrices", J. Phys. Chem. A, **102**, 6220 (1998).
3. K.R. Hobbs and R.D. Coombe, "A Low Energy Method for the Deposition of BN Thin Films", J. Appl. Phys., **87**, 4586(2000).
4. R.H. Jensen, A. Mann, and R.D. Coombe, Energy Transfer from $N_2(v)$ to ClN_3 and a Kinetic Model for the Chain Decomposition of Chlorine Azide", J. Phys. Chem. A, in press (2000).

In addition, we are currently preparing a manuscript describing our work on the near-resonant laser sputtering of Zn and the TECT mechanism, for submission to Applied Physics Letters.

PERSONNEL

Principal Investigator: Professor Robert D. Coombe

Senior Research Collaborators:

Professor Julanna V. Gilbert (University of Denver)
Dr. Amy J. Ray Hunter (Physical Sciences, Inc.)

Graduate Research Associates:

Christopher J. Linnen (MS 1996, currently research staff, Rockwell International Science Center)
Roy H. Jensen (MS 1999, currently a doctoral candidate at the University of Victoria)
Ahmed Soliman (MS 1999, currently a doctoral candidate at Purdue University)
Keith R. Hobbs (current doctoral candidate at DU)

Undergraduate Research Associates:

Aaron Mann (BS 1997, currently a doctoral candidate at the University of California, Berkeley)

REFERENCES

1. T.L. Henshaw, G.C. Manke II, T.J. Madden, M.R. Berman, and G.D. Hager, AFOSR Molecular Dynamics Contractors Review, Waltham, MA, 2000.
2. A.T. Pritt, Jr., and R.D. Coombe, Int. J. Chem. Kinetics, **12**, 741(1980); A.T. Pritt, Jr., D. Patel, and R.D. Coombe, J. Mol. Spectrosc., **87**, 401(1981).
3. D.J. Benard, M.A. Chowdhury. B.K. Winker, T.A. Sedar, and H.H. Michels, J. Phys. Chem., **94**, 7507(1990).
4. D.B. Exton, J. V. Gilbert, and R.D. Coombe, J. Phys. Chem., **95**, 2692(1991).
5. A.J.Ray and R.D. Coombe, J. Phys. Chem., **99**, 7849(1995).
6. R.L. Mulinax, G.S. Okin, and R.D. Coombe, J. Phys. Chem., **99**, 6294(1995).
7. S. Nakamura, M. Senoh, S. Nagahama, N. Iwasa, T. Yamada, T. Matsushita, H. Kiyoku, and Y. Sugimoto, Japan J. Appl. Phys., **35,** L217(1996).
8. Z. Liu, M.P. Gelinas, and R.D. Coombe, J. Appl. Phys., **75**, 3098(1994).
9. AZFOSR Grant No. AFOSR-90-0259.
10. AFOSR Grant No. F49620-93-1-0631
11. K.Y. Du and D.W. Setser, J. Phys. Chem., **96,** 2553(1992).
12. J. Habdas, S. Wategaonkar, and D.W. Setser, J. Phys. Chem., **91**, 451(1987).
13. D Yarkony, J. Chem. Phys., **86**, 1642(1987).
14. T.L. Henshaw, S.D.Herrera, and L.A. Schlie, J. Phys. Chem.A, **102**, 6239(1998).
15. G.C. Manke II and D.W. Setser, J. Phys. Chem. A, **102**, 153(1998).

16. X. Liu, M.A. MacDonald, and R.D. Coombe, J. Phys. Chem., **96**, 4907(1992).
17. K.B. Hewett, G.C. Manke II, D.W. Setser, and G. Brewood, J. Phys. Chem. A, in press (2000).
18. T.L. Henshaw, S.D. Herrera, G.W. Haggquist, and L.A. Schlie, J. Phys. Chem. A., **101**, 4048(1997).
19. A.J. Ray and R.D. Coombe, J. Phys. Chem. **98**, 8940(1994); D.J. Benard, J. Appl. Phys., **74,** 2900(1993).
20. W.A. Rosser, A.D. Wood, and E.T. Gerry, J. Chem. Phys., **50**, 4996(1969).
21. R.D. Sharma and C.A. Brau, J. Chem. Phys., **50**, 924(1969).
22. R.D. Coombe, D. Patel, A.T. Pritt, Jr., and F.J. Wodarczyk, J. Chem. Phys., **75**, 2177(1981).
23. R.D. Coombe and M.H. Van Benthem, J. Chem. Phys., **81**, 2984(1984).
24. R.H. Jensen, A. Mann, and R.D. Coombe, J. Phys. Chem, in press (2000).
25. C.J. Linnen and R.D. Coombe, J. Phys. Chem. B, **101**, 1602(1997).
26. A.P. Baronavski, R.G. Miller, and J.R. McDonald, Chem.Phys., **30**, 119(1978).
27. C.J. Linnen and R.D. Coombe, Appl. Phys. Lett., **72**, 88(1998).
28. J.M. Frisch, G.W. Trucks, M. Head-Gordon, P.M. Gill, M.W. Wong, J.B. Foresman, B.G. Johnson, H.B. Schlegel, M.A. Robb, E.S. Repogle, R.Gomperts, J.L. Andres, K. Raghavachari, J.S. Binkley C. Gonzalez, R.L. Martin, D.J. Fox, D.J. DeFrees, J. Baker, J.J. Stewart, and J.A. Pople, GAUSSIAN 94, Gaussian, Inc., Pittsburgn, PA, 1994.
29. L. Andrews, P. Hassanzadeh, T.R. Burkholder, and J.M.L. Martin, J. Chem. Phys., **98**, 922(1993).
30. I.A. Al-Jihad, B. Liu, C.J. Linnen, and J.V. Gilbert, J. Phys. Chem. A, **102**, 6220(1998).
31. R.M. Desrosiers, D.W. Greve, and A.J. Gellman, Surf. Sci., **382**, 35(1997).
32. D.J.Kester and R. Messier, J. Appl. Phys., **72**, 504(1992).
33. D.J. Benard, C.J. Linnen, A. Harker, H.H. Michels, J.B. Addison, and R. Ondercrin, J. Phys. Chem. B, **102**, 6010(1998).
34. J.A. Meyer, D.H. Klosterboer, and D.W. Setser, J. Chem. Phys. **55**, 2084(1971); D.H. Stedman and D.W. Setser, Chem. Phys. Lett., **2**, 542(1968).
35. K.R. Hobbs and R.D. Coombe, J. Appl. Phys., **87**, 4586(2000).
36. F.W. Byron, M.N. McDermott, R. Novick, B.N. Perry, and E.B. Salomon, Phys. Rev. A, **134**, 47(1964).
37. H. Umemoto, A. Masaki, and S. Sato, Chem. Phys., **141**, 457(1990).
38. Y. Tamir and R. Shuker, J. Appl. Phys., **68**, 5415(1990).